JOURNAL OF MATERIALS SCIENCE 1 (1966) 170–185

Easy Direction Coercive Force associated with Domain Wall Motion in Nickel-Iron Films

J. C. BRICE, J. A. CUNDALL, A. P. KING
Mullard Research Laboratories, Redhill, Surrey, UK

Received 2 February 1966

The origin of domain coercive force in thin nickel-iron films is of considerable scientific and technological interest. Three principal causes of domain coercive force have been suggested. These are surface roughness, inclusions, and the presence of magnetisation ripple in the films. The current theories of these contributions are outlined, and the results obtained experimentally are compared with those expected theoretically. On the basis of this comparison, it appears that all three contributions can be important. However, it is not clear how the components due to the various causes should be combined.

1. Introduction

Domain wall motion plays an important part in magnetisation reversal processes in bulk nickel-iron alloys. The coercive force is defined as the magnetic field required to move an existing domain wall across a specimen. For bulk samples of nickel-iron alloy containing 78 wt % nickel, this field is typically 0.07 Oe. In thin film specimens, the coercive force is much larger (typically about 1 Oe for films of comparable composition, 1000 Å thick). The reasons for this increase are of great scientific interest. In thin films, effects due to the surface become very important and, in addition, the distribution of magnetisation (magnetisation ripple) [1, 2] is peculiar to the thin film state. Domain walls in thin films can occur with different distributions of magnetisation to those found in the bulk state.

Thin films of permalloy prepared in a magnetic field are known to possess uniaxial anisotropy in the plane of the film [3]. The magnetisation in thin films can be reversed by a *coherent rotation* process which is intrinsically fast [4] (typically 2×10^{-9} sec). This makes them suitable for use as computer storage elements [5-8], as this rotation is much faster than the *domain wall migration* process which takes about 5×10^{-7} sec in current ferrite memory elements. From a technological viewpoint, an understanding of the mechanisms responsible for the coercive force is desirable, to ensure that reversal does in fact take place in the memory elements of a store by rotation and that the stray fields present will not cause destruction of the stored information by domain wall movement.

This paper describes the theories of domain coercive force and their application to thin films. It also gives some account of the measurements made in various laboratories, including the authors' laboratory, of the easy direction coercive force and attempts to reconcile the theories with the experimental observations. The paper covers polycrystalline films in the composition range from about 55 to 100 wt % nickel, but the major part of the work discussed has been done on films containing about 82 wt % nickel because this composition appears to be most suitable for computer storage applications. Techniques for measuring coercive force are not discussed since they have been described elsewhere [9].

1.1. Domain Walls in Thin Films

In bulk magnetic material, the domain wall separating regions with different directions of magnetisation is of the Bloch type depicted in fig. 1, in which the spins rotate in the plane of the

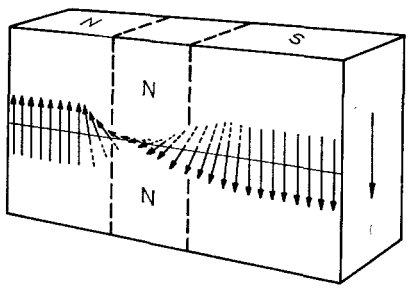

Figure 1 Magnetisation vectors in a 180° Bloch wall.

domain wall. Bloch walls are also found in nickel-iron films greater than about 900 Å thick. The demagnetisation energy of the free poles on the surface of the film due to this type of wall increases as the thickness of the film decreases. In very thin films therefore, a different type of wall becomes energetically more favourable. This is the Néel wall [10] shown in fig. 2, in

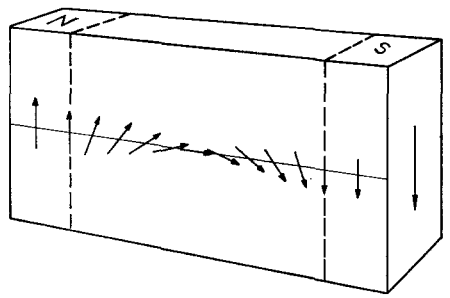

Figure 2 Magnetisation vectors in a 180° Néel wall.

which the magnetisation rotates out of the plane of the wall, i.e. in the plane of the film. Thus, free poles on the film surface are avoided and their demagnetisation energy is reduced at the cost of a small increase in internal wall energy, the total wall energy being reduced. In the intermediate thickness range (500 to 900 Å for alloys containing about 80 wt % nickel), a hybrid wall is energetically favourable. This is the cross-tie wall [11] shown in fig. 3.

The energy of these three types of walls can be calculated approximately by assuming a particular magnetisation configuration and adding the contributions from the exchange, anisotropy and demagnetising energies. The demagnetising energy is difficult to calculate exactly for most models of the magnetisation distribution. Néel [10] has made the approximation that the demagnetising energy can be calculated by treating the wall as an elliptical cylinder whose axes are of a length equal to the wall width and

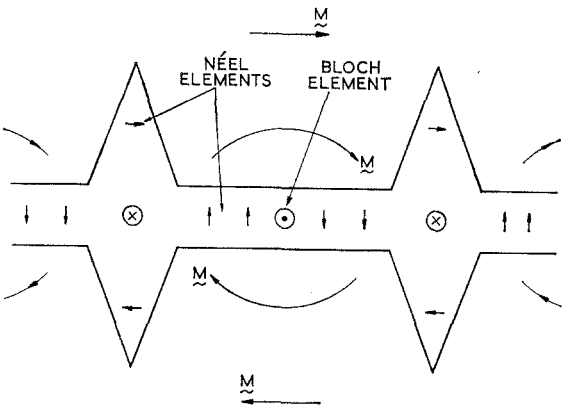

Figure 3 Plan view of a cross-tie wall.

the film thickness. The expression for the wall energy may be minimised with respect to the wall width and both the energies and widths of the domain walls expressed as functions of film thickness. This type of approach has been applied to Bloch walls [10, 12], to Néel walls [10, 12], and to cross-tie walls [12, 13], although in the latter case the analysis was less satisfactory. The energy of different types of domain walls may then be used as a starting point in the calculation of coercive force, as will be seen later.

2. Theories of Domain Coercive Force

The coercive force, H_c, is usually defined for theoretical purposes as the field necessary to move the domain wall over the largest potential energy gradient in its path. This definition implies that the energy gained by moving unit length of wall through an increment of distance dx (which is $2H_cM_sDdx$, where M_s is the saturation magnetisation and D is the film thickness) must always be equal to, or greater than, the change in domain wall energy per unit length dE, so that

$$2H_cM_sD = \left(\frac{dE}{dx}\right)_{max} \quad (1)$$

In its most general form equation 1 can be written [14]

$$H_c = \frac{1}{2M_sD}\left\{\sum\left[\frac{\partial E}{\partial P_i}\frac{dP_i}{dx}\right]\right\}_{\text{max value}} \quad (2)$$

where the P_i are any of the parameters – thickness, magnetisation, exchange energy or anisotropy energy.

Theoretical treatments of coercive force may

be divided into the following three categories:

Firstly, theories in which the coercive force is due to the interaction of the domain walls with non-magnetic inclusions in the material. These have chiefly been developed for bulk materials but are capable of extension to thin films [15].

Secondly, those involving a roughness of the specimen surface [16, 17]. These are important only if the amplitude of the roughness is comparable to the specimen dimensions, and hence, in general, are only applicable to thin films.

Finally, those derived from magnetisation ripple theory [18-20] which are peculiar to thin polycrystalline films.

The models used and assumptions made in deriving the coercive force in these theories will be described, and the predictions of the theories will be discussed with particular reference to the composition and thickness dependence.

2.1. Inclusion Theories

Several workers [21-26] have investigated theoretically the effect of non-magnetic inclusions on the coercive force in bulk materials. The inclusions affect the domain wall energy both because they act as holes in the ferromagnetic material, and because they change the magnetisation distribution in the region of the inclusion.

For small inclusions, it is possible to treat the inclusion as a magnetic dipole formed from the pole density on either end. For inclusions of dimensions large compared with the wall width, this treatment is no longer valid. In this case, small spike domains [22] of reverse magnetisation form round such inclusions, and the movement of the domain wall past an inclusion is in general quite complicated.

Dijkstra and Wert [23] have made calculations of the contribution to the coercive force due to the effect of the holes and to the changes in the magnetisation. They assumed that the domain wall was either rigid and plane or had only small curvatures. This condition is most likely to be fulfilled if the material contains a large number of very small inclusions. This theory predicts a dependence of H_c on the square root of the number of inclusions per unit volume, n, in the matrix. By allowing for the reduction of energy due to the bending of a domain wall, Dietze [24, 25] obtained a relation which gives H_c directly proportional to n.

It would appear that the rigid wall model of Dijkstra and Wert [23] should be valid for a large density of very small inclusions (about 10 to 50 Å diameter) and therefore $H_c \propto \sqrt{n}$. As the inclusion diameter is increased (and the number of inclusions decreased for a constant volume fraction of impurity), the dependence of H_c on n should change so that the coercive force becomes proportional to n as predicted by Dietze. Although the form of the expression for coercive force would be expected to change as the inclusion diameter becomes large compared with the wall width (when reverse Néel spike domains form), the coercive force would still be expected to be directly proportional to n. This behaviour would be expected until the volume fraction also increased to such an extent that the distance between inclusions became less than the range of the interaction potential of an inclusion in the magnetic matrix.

These theories were originally derived for bulk material but are capable of extension to the thin film case, with similar predictions. Brice [15] has extended the theory of Dijkstra and Wert in this manner with similar limitations and obtained the relation

$$H_c = \frac{1.4\gamma}{M_s}\left[\frac{nd^6}{q^3 w D}\log_e\left(\frac{2l}{q}\right)\right]^{\frac{1}{2}} \qquad (3)$$

in which γ is the wall energy per unit area, q is the wall width, d the inclusion diameter (where $q \gg d$), and l, D and w are the length, thickness and width of the specimen, respectively. For constant inclusion diameter and concentration, the compositional and thickness dependence of coercive force are shown on figs. 4 and 5. Equa-

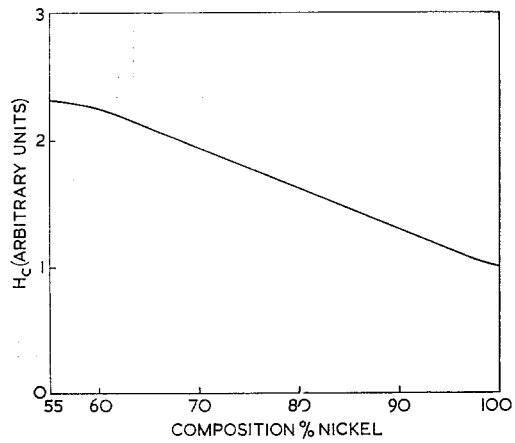

Figure 4 The compositional dependence of coercive force on the inclusions theory [39]. (Inclusion diameter = 100 Å; film thickness = 1000 Å; width and length of domain = 0·05 cm.)

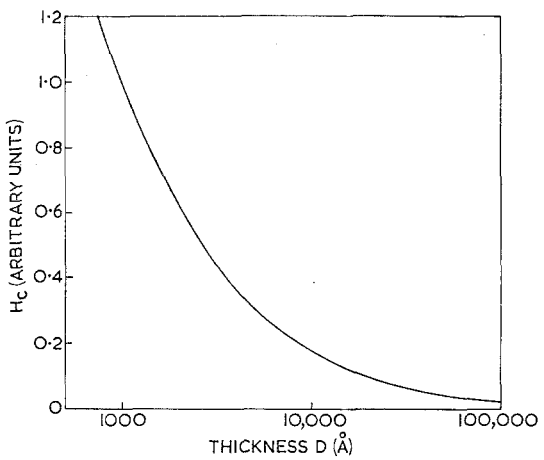

Figure 5 The thickness dependence of coercive force on the inclusions model [39]. (Inclusion diameter = 100 Å; composition = 80/20 Ni/Fe; width and length of domain = 0·05 cm.)

tion 3 is derived for a mechanism in which a decrease of wall energy is incurred by removal of part of the wall. An alternative mechanism which has a much smaller effect on the coercive force involves the production of dipoles at the inclusions.

Nix and Huggins [26] have treated the coercive force due to large inclusions in single crystal material by numerical rather than analytical methods. They followed the statistical arguments of Dijkstra and Wert but with less justification, because for large inclusions only a few cut the domain wall at any given position. An electron microscopic investigation of the effect of large inclusions on the movement of cross-tie walls [27] has shown that the coercive force can be expressed in the phenomenological relation

$$H_c \sim (1.2\gamma_{ct} + 0.25\ K_u t)n_l/M_s \qquad (4)$$

where K_u is the anisotropy constant, n_l is the number of interactions with inclusions per unit length, γ_{ct} is the cross-tie wall energy per unit area, and t is the average separation of the inclusion from the nearest cross-tie. The composition and thickness dependence of the energy of cross-tie walls is known only on the basis of approximate models due to Prutton [13] and to Huber, Smith and Goodenough [11]. The compositional dependence of coercive force calculated on these bases depends on the relative magnitudes of the two terms in equation 4. Reasonable assumptions made for t infer that the second term is usually negligible compared with the first term, and therefore the composition dependence follows that of $1/M_s$.

2.2. Surface Roughness Theories

Films possessing a surface roughness will exhibit a positional dependence of film thickness and therefore of domain wall energy. The coercive force, that is the applied field required to move the wall past a point at which the rate of change of wall energy is a maximum, may be found from equation 1 if the dependence of domain wall energy on thickness is known. This assumes [16] that the surface structure is of the form of a surface ripple with peaks and troughs lying in the direction of magnetisation, so that there are no free poles on the surface. The separation of the peaks and troughs must be large compared to the domain wall width because the calculation of domain wall energy is valid only when the film has a constant thickness throughout the width of the domain wall.

For the Néel model of the Bloch wall, the coercive force is given by

$$H_c = \frac{S}{2DM_s}\left[\frac{A\pi^2}{q} + \frac{K_u q}{2} + \frac{\pi M_s^2 q^3}{(q+D)^2}\right] \qquad (5)$$

where q is the domain wall width, A is the exchange constant, and S, the surface roughness, is defined as the maximum rate of change of film thickness with position in the film plane.

Inserting the experimental values of K_u, M_s and A for nickel-iron films in the composition range 55 to 100 wt % nickel into the above, this expression reduces to the form

$$H_c = H_0 D^{-4/3} \qquad (6)$$

Behringer and Smith [17] have modified Néel's theory by making a more detailed calculation of the demagnetising energy of the domain wall, using a different arbitrary configuration of the magnetisation direction as a function of distance from the wall centre. Their expression for the coercive force

$$H_c = \frac{S}{4M_s D}\left[25.32\frac{A}{q} + 0.695\ K_u q + 0.8365\frac{M_s^2 q^2}{D}\right] \qquad (7)$$

is very similar to that calculated using the Néel model.

This expression also reduces to $H_c = H_0 D^{-4/3}$ for typical values of A, K_u and M_s found in nickel-iron films.

The model of a Néel wall [10] which occurs in films thinner than about 600 Å can also be used to find the coercive force on the surface roughness model. The resulting equation is

$$H_c = \frac{S}{2DM_s}\left[\frac{A\pi^2}{q} + \frac{K_u q}{2} + \frac{\pi q D(2q + D)\, M_s^2}{(q + D)^2}\right] \quad (8)$$

Here the thickness dependence of the coercive force is more complicated than for Bloch walls, as the first and third terms within the brackets of equation 8 are of comparable magnitude, and the thickness dependence of the wall width does not reduce to a simple D^n power law within the whole of the thickness range of interest. The calculated dependence of the coercive force as a function of thickness for several compositions is shown in fig. 6. Arbitrary units have been used

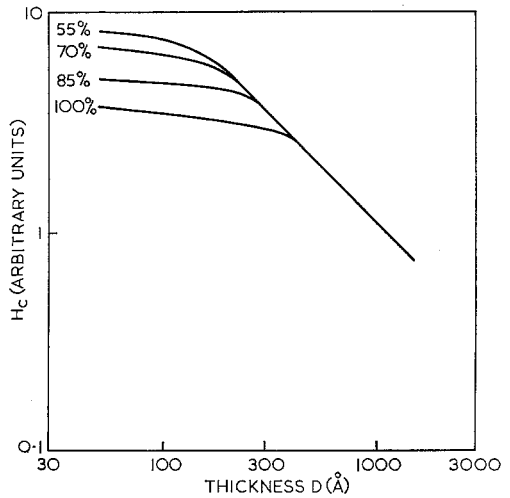

Figure 6 The dependence of coercive force on thickness and composition for Néel walls derived from equation 8 for various nickel contents.

for H_c because of the uncertainty in the value of S. At thicknesses greater than a critical thickness, which depends on composition, the coercive force is inversely proportional to thickness and independent of composition. There is an initial flat portion of the curves where the coercive force is nearly independent of thickness and the length of this region varies with composition. Note that the results have been calculated to beyond the thickness at which Néel walls are known to be replaced by cross-tie walls. For small film thicknesses, the coercive force decreases with increasing nickel content.

It has been shown, both experimentally by Fuchs [2] and theoretically by Collette [28] and Brown and La Bonte [29], that the magnetisation distribution across the Néel wall assumed in the derivation of relation [8] is incorrect. The actual distribution is not however amenable to analytical calculation.

An expression derived by Middelhoek [12] for the energy of cross-tie walls can be used to calculate the coercive force in the region 500 to 900 Å, where this type of domain wall occurs. In this case, one obtains, after several approximations,

$$H_{c\ (\text{cross-tie walls})} = 0.6\, H_{c\ (\text{Néel walls})} \quad (9)$$

Here $H_{c\ (\text{cross-tie walls})}$ has the same thickness dependence as $H_{c\ (\text{Néel walls})}$, i.e. inversely proportional to thickness in this film thickness region. Another expression derived by Prutton [13] for the cross-tie wall energy, based on a different model of the magnetisation distribution, can be shown to produce a relation of the form

$$H_c = \frac{3S}{2D}\sqrt{(2\pi A)} \quad (10)$$

In this case, the coercive force is also inversely proportional to the thickness and independent of composition (the compositional dependence of A is small [30]).

The expressions for the coercive force due to surface roughness give a monotonic increase with nickel content for Bloch walls, whilst for Néel walls and both models of the magnetisation distribution of the cross-tie wall, the coercive force is independent of film composition.

These surface roughness theories are limited in so far as the approximations require that the period of the roughness must be considerably greater than the domain wall width. Nevertheless, they can be used to predict the compositional dependence of coercive force. The coercive force is shown in arbitrary units on fig. 7 for the models described above. It has been assumed that the surface roughness is constant in period and amplitude for films of varying thickness and composition.

There appears to be no report in the literature of the extension of these calculations to derive the temperature dependence of the coercive force. In principle, the variation of coercive force with sample temperature, for the surface roughness model, could easily be obtained from

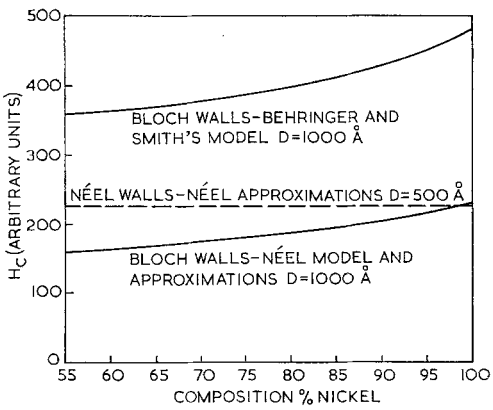

Figure 7 The compositional dependence of coercive force on various surface roughness theories.

these expressions using the known temperature dependences of K_u, A, and the other parameters involved.

The theoretical approach would have to be considerably modified to take account of magnetic pole distributions other than those due to the presence of a domain wall. Such pole distributions may occur on surface irregularities such as "bumps" due to an uneven substrate (see for example fig. 8, which is an electron micrograph of a replica of a film on an uneven substrate).

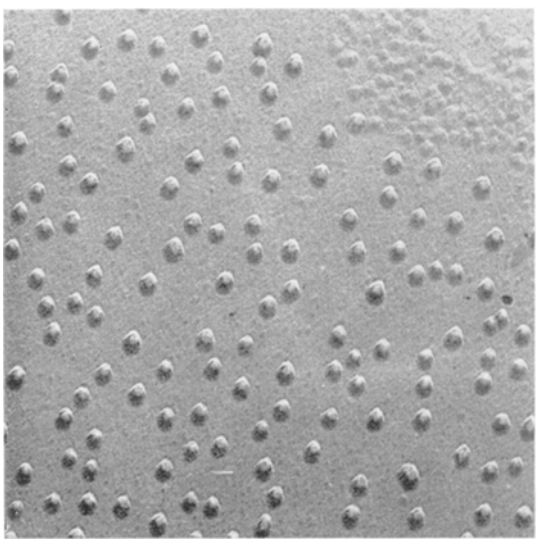

Figure 8 Electron micrograph of a replica of the surface of a nickel-iron film on a glass substrate.

2.3. Ripple Theories of Coercive Force

Various workers [1, 2] have shown that the magnetisation in polycrystalline thin films is not completely parallel as was first predicted for films of thickness less than about 3000 Å [31]. The magnetocrystalline anisotropy energy from randomly-orientated crystallites in combination with the exchange energy causes slight local variations of the magnetisation direction about the mean direction. For films containing between about 66 to 86 wt % nickel [32, 33], these deviations are usually small, and typically 90 wt % of the magnetisation is deviated less than a few degrees from the mean direction. The amount of local deviation depends on stresses in the film [34, 35], grain size [36], preferred orientation [37], composition [37], the magnetic field applied during preparation [38, 39], and, for evaporated films, the angle of incidence of the vapour beam on the substrate [40].

Variations in the direction of local magnetisation at right angles to the mean easy direction are, in general, smaller than those parallel to the easy direction (fig. 9). The resultant magnetisation structure tends to adopt a wave-like formation from which the name magnetisation ripple is derived. This phenomenon has been investigated by the technique of Lorentz electron microscopy [1], in which variations in the magnetisation directions cause corresponding deviations of the electron beam which show as intensity variations on electron micrographs.

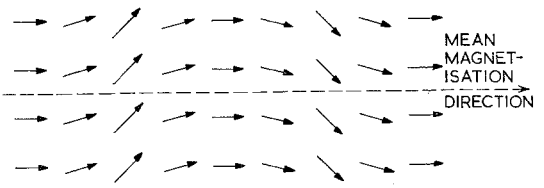

Figure 9 Magnetisation vectors in magnetisation ripple model.

Rother [18] has calculated the coercive force for a Néel wall in his series of papers on magnetisation ripple. His earlier treatment of magnetisation ripple has been corrected [41], and Joenk [19] has used Rother's revised ripple theory [41], which is only valid for small angular deviations of the magnetisation direction, to derive the equation

$$H_c = \frac{0.298\ K_u^{\frac{1}{2}}\ K_\sigma\ a}{M_S^{\frac{3}{2}}\ A^{\frac{3}{2}}\ D^{\frac{1}{2}}} \left[\frac{8A/b\ (\sin\nu + 0.4\cos\nu) + M_S^2\ D}{\sqrt{\{2A + 12M_S^2 D\ (q - D/3)\}}}\right] \quad (11)$$

where $K_\sigma = K_1 + \frac{1}{2}\sigma\lambda_s$,* in which K_1 is the magnetocrystalline anisotropy constant, σ is the stress, and λ_s is the appropriate average of the magnetostriction constants λ_{111} and λ_{100}, b is the mean ripple wavelength ($\simeq$ 10 times the crystallite size), and ν is the angle between the easy axis and the domain wall. Figs. 10, 11 and 12 show the variation of coercive force with composition, thickness and crystallite size expected from both this expression and that due to Rother for films with zero local stress.

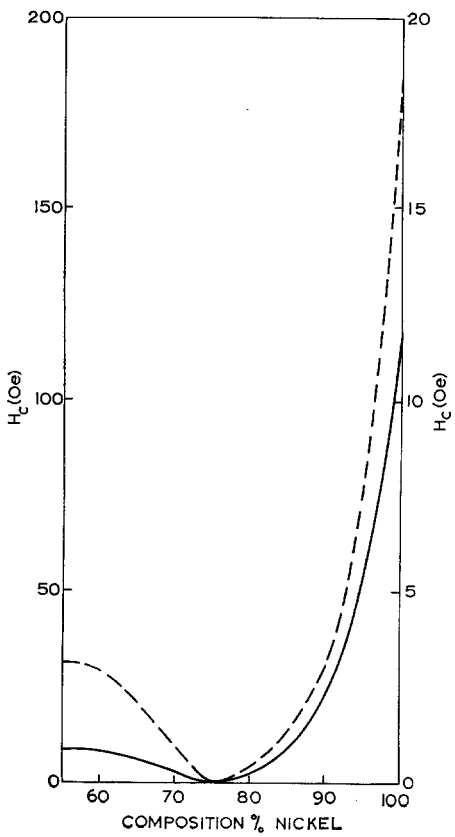

Figure 10 The variation of coercive force with composition. (Curve —— from equation 11 (0 to 20 scale); - - - - from Rother's theory (0 to 200 scale); the crystallite diameter has been taken to be 260 Å; the film thickness 500 Å.)

3. Experimental Observations

The major difficulty in correlating coercive force data with theoretical studies is that in most experiments the variation of one experimental parameter involves the simultaneous variation

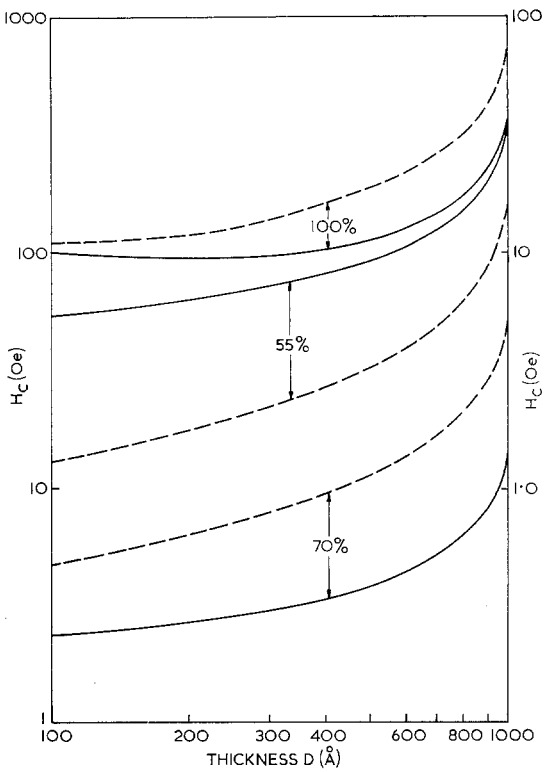

Figure 11 The variation of coercive force with film thickness for several compositions. (Curve —— from equation 11 (0·1 to 100 scale); - - - - from Rother's theory [18] (1 to 1000 scale); the crystallite size was taken to be 260 Å.)

of several properties. For example, increasing the substrate temperature results in changes in the uniaxial anisotropy [42], the grain size [43-45], and angular dispersion [36, 45]. In the literature, insufficient data is often given concerning relevant parameters; for example, the nature and concentration of inclusions.

Several possible causes of domain coercive force have been discussed, and the dominant one for any film will depend on its particular combination of properties, which in turn will be governed by the preparation conditions. For example, the amount of non-magnetic material included in evaporated films is influenced by the ratio of pressure to deposition rate [46].

A large proportion of the published work has been concerned with the thickness dependence of coercive force. This emphasis is perhaps due to the $-\frac{4}{3}$ power law predicted by Néel [16] (equation 6). Experiments have covered a

*A different expression for K_σ can be derived from the work of Lee [79]. This suggests a smaller contribution due to stress.

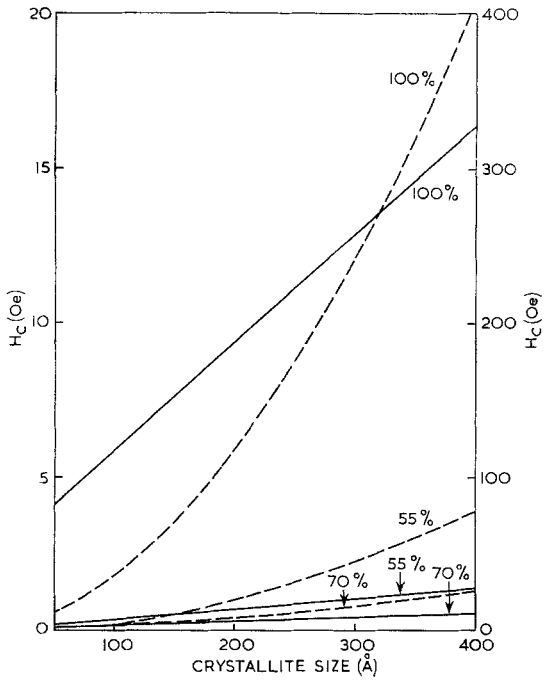

Figure 12 The dependence of coercive force on crystallite size for 500 Å thick films for several compositions. (Line —— from equation 11 (0 to 20 scale); - - - - from Rother's theory [18] (0 to 400 scale).)

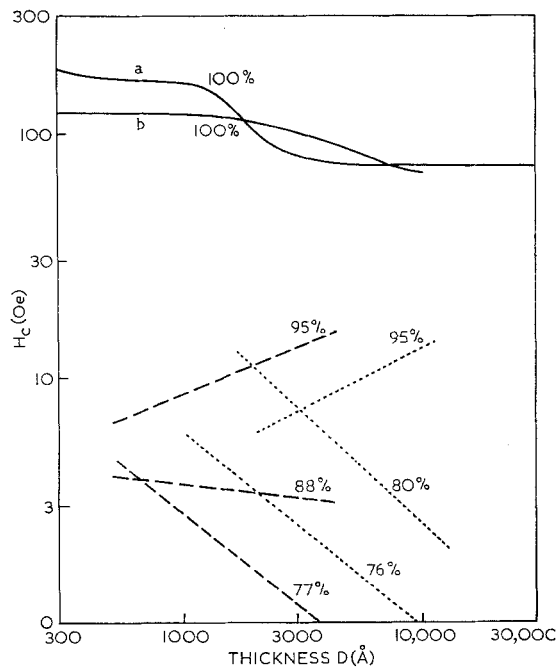

Figure 13 The dependence of coercive force on film thickness for electrodeposited films of various nickel contents. (Curve a from Reimer [51], b from Ruske [52]; - - - from Wolf [48]; . . . . from Lloyd and Smith [49].)

wide thickness range (100 Å to several microns) for both electrodeposited and evaporated films. Much of the initial work was concerned with electrodeposited films but the emphasis of more recent work has been on evaporated films.

3.1. Electrodeposited Films

For electrodeposited films thicker than about 1000 Å, it has been found [47-50] that the results can often be represented by

$$H_c = H_0 D^{-n} \qquad (12)$$

where the exponent, n, depends on composition. Some results showing this compositional dependence are given in fig. 13 together with those of Reimer [51] and Ruske [52] on pure nickel, which cannot be fitted to a simple power law. Reimer deposited his films on metallic substrates with various sizes of grain in the substrate and found that both the magnitude of H_c and the form of the thickness dependence of H_c were strongly dependent on the type of substrate used.

The variation of the exponent, n (equation 12), with composition [48, 50] is shown in fig. 14. In most cases, n is less than the $\frac{4}{3}$ predicted by

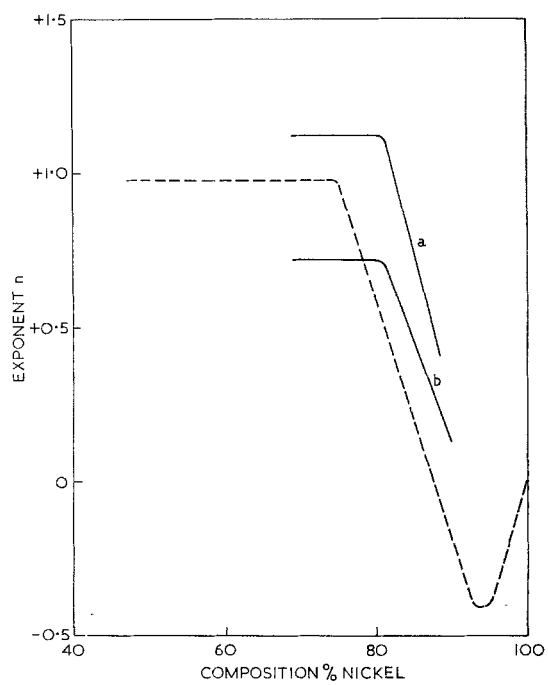

Figure 14 The dependence of the exponent n on composition for electrodeposited films. (Curve a – plating bath with saccharin; b – plating bath without saccharin; —— Uehara [50]; - - - Wolf [48].)

Néel's surface roughness theory and even becomes negative at high nickel content. It is known that the surface roughness of electrodeposited films increases with thickness [47] due to the formation of a depletion layer near the cathode. This would be expected to alter S (i.e. $(dD/dx)_{max}$) in equations 5, 7 and 8, and make S a function of thickness. This would probably mean that the coercive force would decrease less rapidly with increasing thickness than the $D^{-4/3}$ relation predicted by Néel, which is in accord with the observations.

The effects of various sorts of surface roughness have been considered in detail by Lloyd and Smith [47] for electrodeposited films. Their results should also be applicable to evaporated films. They suggested a division into three types of surface roughness:

(a) That which has the wavelength of the roughness of the same order as the domain wall width; possibly caused by either grains in the substrate or film, or the depletion layer near the cathode.

(b) That which has a wavelength large compared with the wall width and an amplitude small compared with the film thickness; probably due to undulations of the surface of the substrate.

(c) That which has a period and amplitude large compared with the film thickness; this is usually obtained by special roughening of the substrate surface.

It was found that types (a) and (b) affect the value of the n in equation 12, whereas type (c) has little effect on n but causes an increase in H_0. Reimer [51] has also shown that for both electroplated and evaporated films increasing the substrate grain size, probably type (a) roughness, causes an increase in the coercive force.

Several workers have shown that the domain coercive force is strongly dependent on composition [48-50]. The results obtained agree fairly closely in shape (see fig. 15). Both the curves shown in this figure give a rapid rise in H_c with nickel content for nickel contents greater than about 90 wt %.

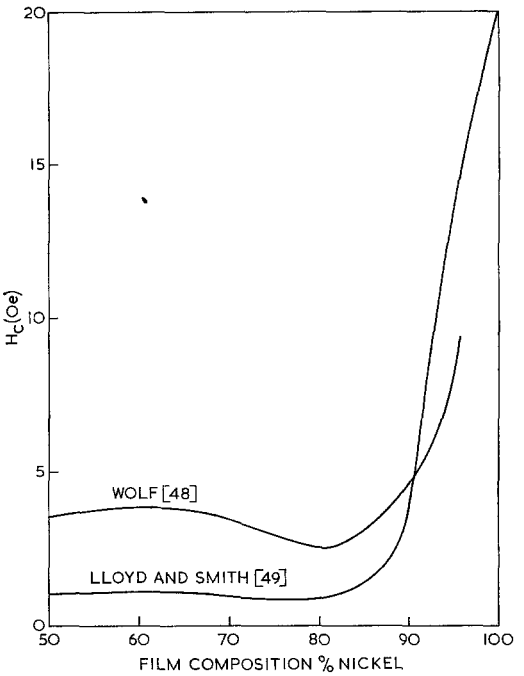

Figure 15 Compositional dependence of coercive force for electrodeposited films.

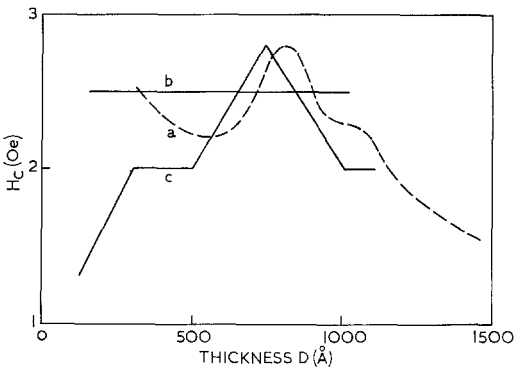

Figure 16 The variation of coercive force with film thickness for evaporated films containing about 81% wt nickel. (Curve 5 – Methfessel, Middelhoek and Thomas [59]; b – Behrndt [56] $p/r = 3 \times 10^{-7}$ torr sec/Å; c – Behrndt [56] $p/r = 5 \times 10^{-5}$ torr sec/Å, where p = pressure and r = deposition rate. Curves b and c correspond to measurements made at 200°C.)

3.2. Evaporated Films

For evaporated films even greater differences occur between the results of different workers for the variation of coercive force with thickness. Some typical results are shown on figs. 16 and 17. Some workers have reported power laws with various exponents [53-55]; some have found the coercive force to be independent of thickness [56-58]; and others have found maxima [56, 59, 60] in the thickness dependence of the coercive force. It is clear from the widely differing results obtained for very similar film compositions that there must be marked differences in the films themselves. These differences are probably due to the effects of deposition parameters. It has been shown that the more

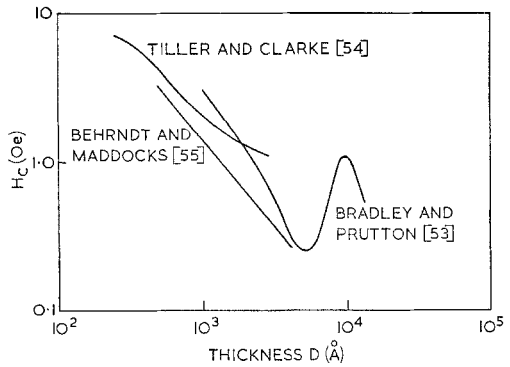

Figure 17 The thickness dependence of coercive force for evaporated films containing about 81 wt % nickel.

important parameters are the partial pressures of gases present during the evaporation [61], deposition rate [45, 56], substrate temperature [45, 62-64], and the pretreatment of the substrate [55, 65]. The partial pressure and the deposition rate control the amount of gaseous material included in the film. The deposition rate [43, 45] and the substrate temperature [36, 43, 44, 64] both affect the grain size. The pretreatment of the substrate will affect the surface roughness of the film.

The effect of the ratio of gas pressure to deposition rate on coercive force has been investigated by Behrndt [56] for pure iron, pure nickel, and the alloy containing 80 wt % nickel. The coercive force was measured using the Kerr effect at intervals during the deposition, with the film still under vacuum and at the deposition temperature of about 200° C. Fig. 16 shows two sets of his results for the 80 wt % nickel alloy together with those of Methfessel, Middelhoek and Thomas [59]; and fig. 18 shows his results for nickel together with those of Hellenthal [63]. These results show that the coercive force is nearly independent of thickness for low values of the ratio of pressure to deposition rate, but for higher values of the ratio a maximum value is found.

The independence of coercive force on thickness has also been noted by Humphrey [57] for films less than 200 Å thick. In addition, Zaveta [58] has found H_c to be independent of film thickness over the thickness range 125 to 7870 Å for iron films, for values of pressure to deposition rate as high as about 10^{-4} torr sec/Å. Freedman [61] has shown that the partial pressure of certain gases is more important than the total pressure. In his work on nickel films, he showed that nitrogen has little effect on

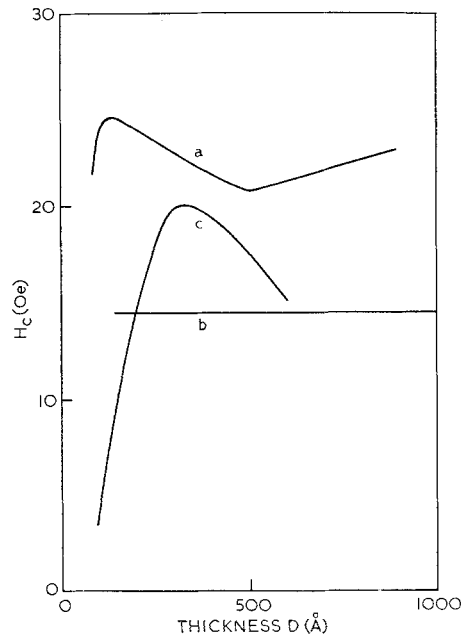

Figure 18 The thickness dependence of coercive force for evaporated nickel films deposited at a substrate temperature of 200°C. (Curve a – Behrndt [56] p/r = 3 × 10^{-5} torr sec/Å; b – Behrndt [56] p/r = 7 × 10^{-9} torr sec/Å; c – Hellenthal [63].)

coercive force, water vapour has some effect, and oxygen a large effect. He attributed the effect to variations in internal stress without indicating the exact mechanism.

By evaporating films with different ratios of pressure to deposition rate, Brice [15] was able to make films with different densities. Films with high ratios had gaseous inclusions and lower densities. It was found that for these films the square of the domain coercive force depended on the film density up to a limiting density above which it was presumed that inclusions were not formed. Assuming that the volume of the inclusions depends on the difference between the film density and the limiting density, the observations (see fig. 19) are consistent with a component of coercive force, being dependent on the square root of the volume of the inclusions.

The effect of increasing the evaporation rate is to cause a decrease in the crystallite size [45]. Independent of any effect on the amount of material included, a change in crystallite size will affect some of the magnetic properties of films including their coercive forces. There is only very sparse evidence on the subject (see however fig. 20). Most workers prefer to change the grain size of films by changing the substrate

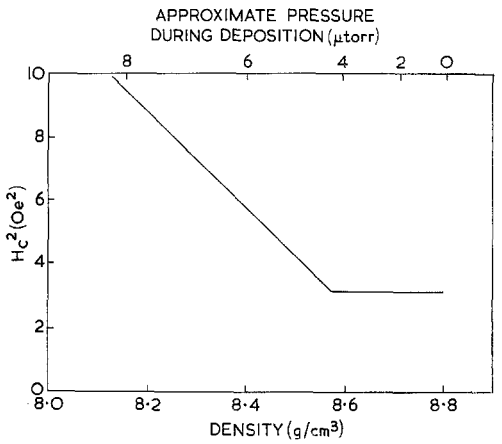

Figure 19 The dependence of coercive force on film density. Films containing 81±1 wt % nickel, deposition rate 8±2 Å/sec.

temperature. Fig. 20 shows how substrate temperature affects coercive force. Changing the substrate temperature however involves changing other parameters; for example, the uniaxial anisotropy [42, 45]. Rother [18] found a linear relation between H_c and $a\sqrt{H_k}$, where a is the

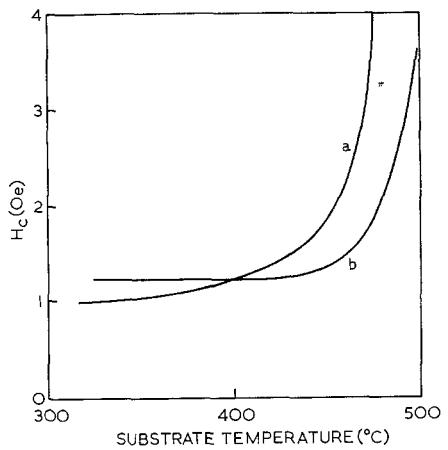

Figure 20 The dependence of coercive force on substrate temperature [45] for films containing 81% wt nickel. (Film thickness was 2000 Å; deposited at evaporation rates of 15 Å/sec, curve a, and 140 Å/sec, curve b.)

grain size. This agrees with his initial formulation of the ripple theory; however, later versions [19] predict that H_c should be proportional to $aH_k^{\frac{1}{2}}$.

The effects of various pretreatments of substrates have been investigated by several workers [55, 64, 65]. Behrndt and Maddocks [55] found that minimum values of coercive force were obtained for films containing 81 wt % nickel by etching away about 5 μm of the glass substrate surface prior to evaporation. Subsequent coating with about 4000 Å of silicon monoxide did not have any marked effect on the average results but did much to decrease the scatter. A similar decrease in scatter has been observed [66] using aluminium substrates coated with silicon monoxide, but in this case the use of an 8000 Å silicon monoxide layer caused a significant (typically 40%) decrease in the coercive force. Similar results were found by Wiehl [64].

The influence of the physical nature of the surface is further shown by the dependence of coercive force on the growth of crystallite chains in evaporated specimens prepared at various angles of incidence, θ_i, of the vapour beam on the substrate. The rapid increase of coercive force with θ_i is accompanied by a decrease in angular dispersion [40] (fig. 21). A similar dependence of coercive force on the angle of incidence has been observed in iron [67] and cobalt [68] films.

Table I summarises the results of varying deposition parameters found for evaporated films.

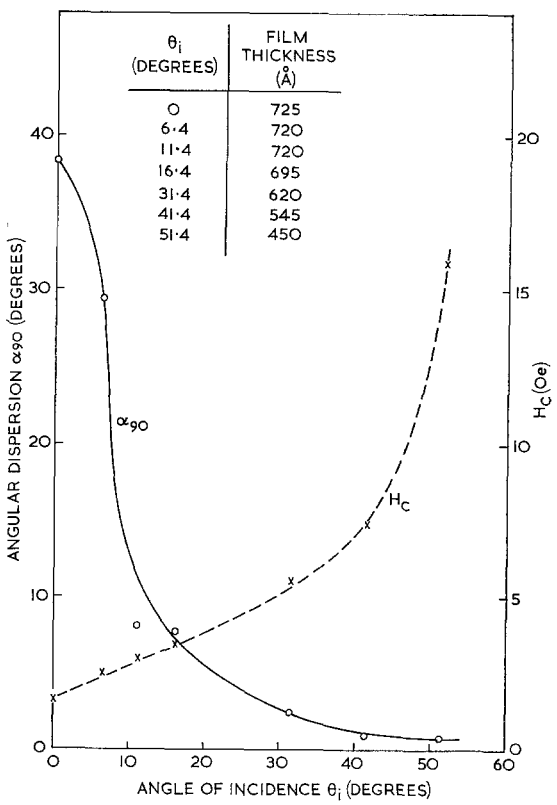

Figure 21 Dependence of coercive force and angular dispersion on the angle of vapour beam incidence for evaporated 75/25 nickel-iron films [40].

TABLE I The effect of deposition parameters on coercive force.

Parameter	Effect on increasing the parameter	
	On domain coercive force	On film structure
Thickness	(a) In high vacuum increase up to 500 Å and is then constant thereafter	For very thick films (10^4 Å) increase grain size
	(b) In poor vacuum exhibits a maximum except in films containing nearly 100 wt % nickel.	
Pressure during deposition	Increase	Increase gas content
Growth rate	Decrease	Decrease grain size and gas content
Substrate temperature	Increase	Increase grain size
Field during deposition	Very small (for applied fields in the range 0 to 30 Oe)	None
Substrate roughness	Increase	Increase surface roughness
Angle of vapour beam incidence	Increase	Chain growth of grains

The dependence of coercive force on composition found by various workers [33, 40, 62, 69] is shown on fig. 22. On this figure, the compositions given for curves a and b are those of the source and for curves c and d that of the film. Because of the differences in the partial vapour pressures of nickel and iron over the melt [70], a film usually contains more iron than the melt [71, 72]. This effect probably accounts for the differences between the sets of results on fig. 22.

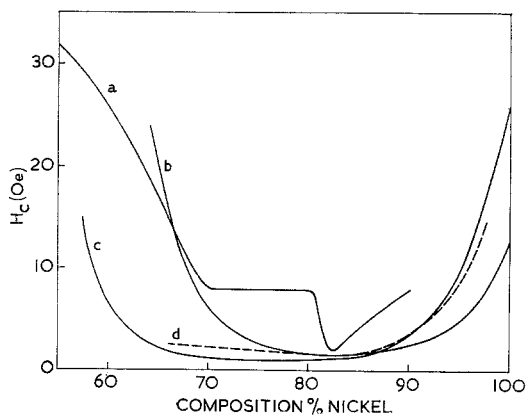

Figure 22 The dependence of coercive force on composition for evaporated films. (Curve a – Blades [62]; b – Raffel and Smith [69]; c – Cundall and King [40]; d – Siegle and Beam [33]; note that for curves a and b the composition is that of the melt, whilst for curves c and d it is that of the film.)

Several authors have investigated the relationship between coercive force and the other magnetic parameters, angular dispersion, α_{90}, and uniaxial anisotropy field, H_k. Thus, measurements on arrays of film elements containing 81 wt % nickel have shown [60] a component of coercive force which was proportional to $\alpha_{90}H_k$. Unpublished results showed that α_{90} was proportional to $H_k^{-0.3}$, giving a relation between H_c and $H_k^{0.7}$. Several authors have reported relations between H_c [73, 74] or (H_c/H_k) [75] and α_{90} (see fig. 23). Pinch and Pinto [34] and

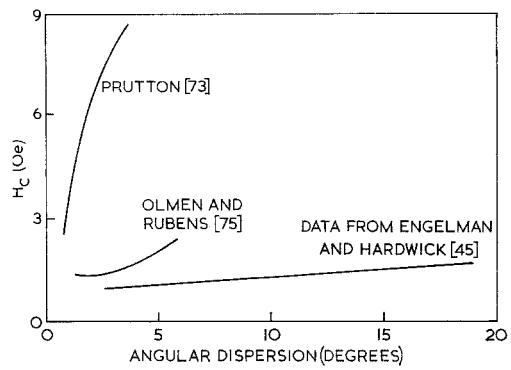

Figure 23 Coercive force as a function of angular dispersion.

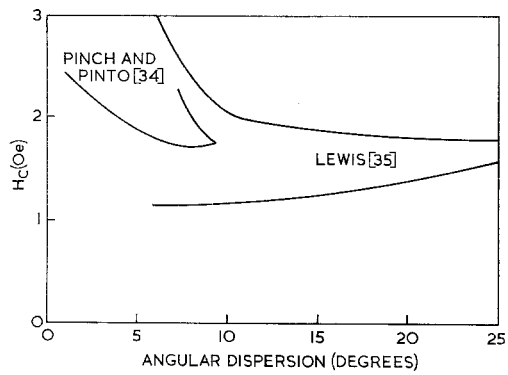

Figure 24 Coercive force as a function of angular dispersion for strained specimens.

Lewis [35] have strained specimens and measured magnetic properties including H_c and α_{90} as a function of applied stress. On fig. 24,

their results are replotted to show the relation between stress-induced variations of coercive force and angular dispersion. Films deposited in increasing magnetic fields have decreasing angular dispersions [38, 40]. Figs. 25 and 26

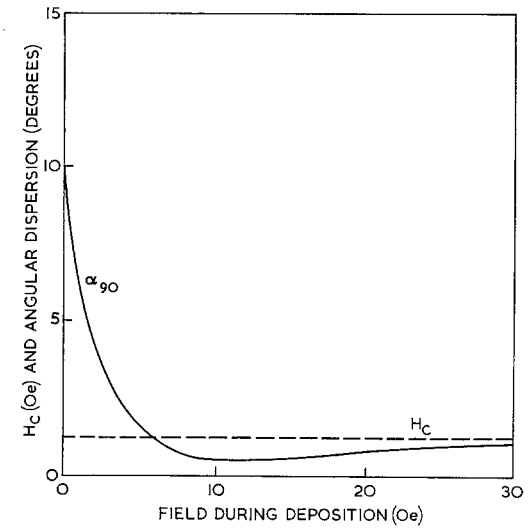

Figure 25 Coercive force and angular dispersion as a function of field during deposition [40] for films containing 77·5% wt nickel. (Film thickness = 1000 Å.)

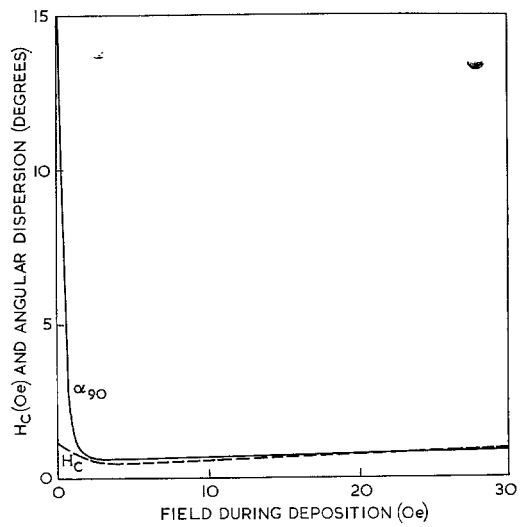

Figure 26 Coercive force and angular dispersion as a function of field applied during deposition [40] for films containing 83% wt nickel. (Film thickness = 800 Å.)

suggest that the coercive force does not depend on deposition field for films containing 77 wt % nickel but may do so for films containing 83 wt %. It seems therefore that H_c and α_{90} are not directly related although they may be related through some third property of the film such as grain size.

The effect of changing the temperature at which the coercive force is measured has not been investigated fully. Van Itterbeek and Dupré [76] have investigated nickel films about 150 Å thick at very low temperatures, and obtained a relation of the form

$$H_c = H_{co} \exp(-B\sqrt{T}) \qquad (13)$$

where T is the absolute temperature, and H_{co} and B are constants.

Hirsch [77] has shown that this type of relation would be expected on the basis of thermally-induced jumps in the magnetisation.

Hellenthal [63] working on thin nickel films in the range 80 to 480° K found an increase in H_c with decreasing temperature, which he attempted to correlate with changes in magneto-crystalline anisotropy. His results are shown in fig. 27.

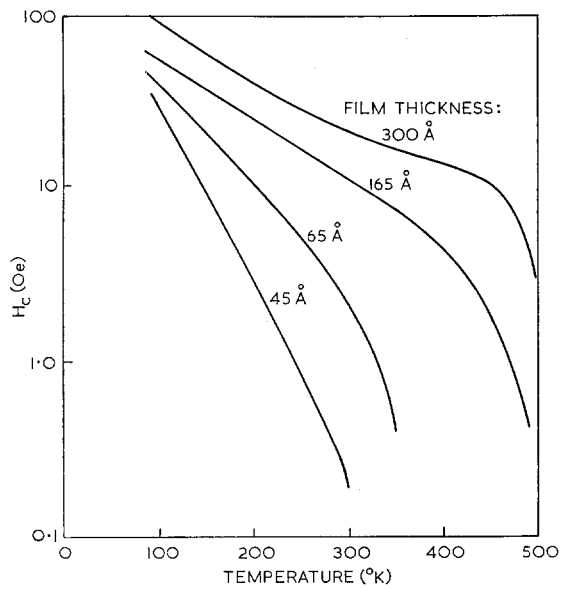

Figure 27 The coercive force of nickel films as a function of measurement temperature [63] for various film thicknesses.

4. Discussion

In the previous section, it was shown that considerable discrepancies in the results of different authors existed. The definition of coercive force used is sometimes inconsistent; thus, some workers use a criterion in which the resultant magnetisation along the easy axis

becomes zero at the coercive force, whilst others quote the field sufficient to move an existing domain wall. The latter is closer to the definition used in theoretical treatments. In addition, for small specimen sizes, the internal demagnetising field may cause complications resulting in an apparent decrease in the coercive force.

The thickness dependence studies of the coercive force have often shown a simple D^{-n} power law relationship for electrodeposited films, but there is less evidence for such a law for evaporated films. There is also the complication of the change in sign of the exponent n with composition for electrodeposited films (see fig. 14).

A negative exponent (i.e. an increase of coercive force with film thickness) would be expected on the surface roughness theories for Bloch walls for large negative anisotropy. This would imply a large uniaxial anisotropy perpendicular to the film plane. The presence of isotropic stresses in the film plane in conjunction with negative values of magnetostriction can give rise to an anisotropy perpendicular to the film plane. The progressive increase in the magnitude of the magnetostriction constant as 100 wt % nickel content is approached would cause increasing anisotropy magnitude and concomitant deviations from the $-\frac{4}{3}$ exponent. The film thickness range in which these effects may occur is affected by the assumptions made in the calculations (see fig. 28), so that it is not surprising that only qualitative agreement can be obtained. In addition, the parameter S has been assumed to be independent of film thickness; this is known to be untrue for electrodeposited specimens [47].

The observations of a maximum in the thickness dependence of the coercive force at thicknesses of 700 to 900 Å for evaporated films have been associated [59] with the thickness range in which cross-tie walls are observed. Fig. 29 shows the density of cross-ties found [59, 78] as a function of film thickness. This coercive force maximum has only been observed in films deposited with a high ratio of pressure to deposition rate for evaporated films [56]. These specimens presumably contain a higher inclusion density than those prepared at lower pressure-to-deposition-rate ratios and which do not show the maxima.

Extension of the inclusion theory for small inclusions [15] to thin films containing Néel walls predicts that the coercive force increases

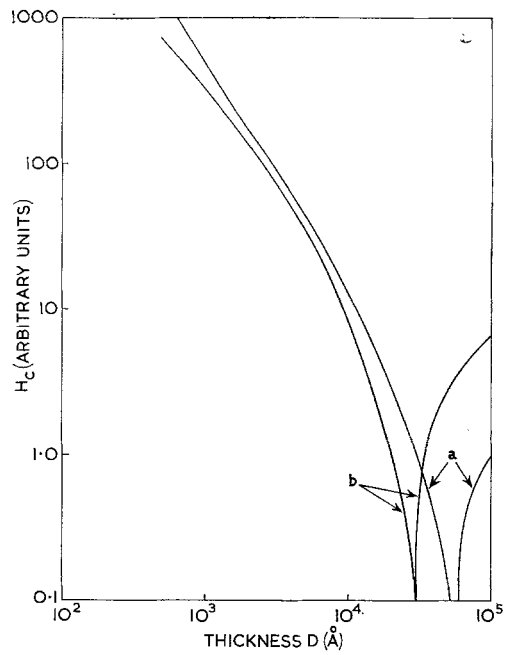

Figure 28 The thickness dependence of coercive force for 80/20 films. (Curve a – Behringer and Smith's model; b – Néel's model of Bloch walls; $A = 1 \times 10^{-6}$ ergs/cm; $M = 1000$ cgs; $K_u = -2 \times 10^5$ ergs/cm^3.)

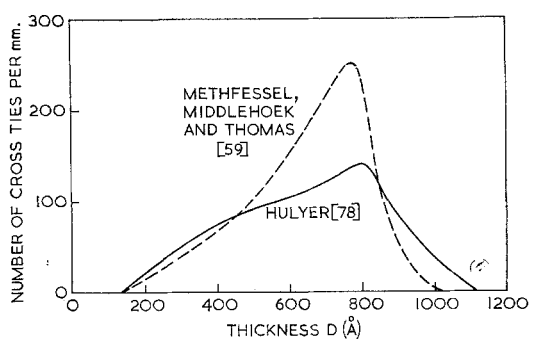

Figure 29 The number of cross-ties per unit length of domain wall in films containing about 80 wt % nickel.

with increasing thickness, whereas for films containing Bloch walls the coercive force would be expected to decrease with thickness, thus conceivably giving a maximum in the thickness range at which the wall structure changes from Néel to Bloch, i.e. the cross-tie wall region.

Wade's phenomenological inclusion theory (equation 4), which involves interactions between large inclusions and cross-ties, predicts a local minimum in the coercive force at the thickness for maximum cross-tie density.

The magnetisation ripple approach predicts

a slight monotonic increase in coercive force with film thickness over the range of validity of the existing calculations, which are applicable only to Néel walls. As the present ripple theory is only valid for small angular deviations of the magnetisation from the mean direction, it will be valid only for specimens possessing small angular dispersions (i.e. the composition range ~ 66 to 86 wt % nickel) [32, 33]. The relatively sparse results in the appropriate thickness range for such specimens show no direct correlation with this theory although the magnitudes predicted are comparable with those observed.

Published work shows that only the ripple theory bears even qualitative comparison with the compositional dependence of coercive force (compare fig. 10 and 22). (At the extremes of the composition range, only qualitative agreement would be expected, because of the known large angular dispersions which make the theory of dubious validity.) The shape of the composition curves appears to be roughly independent of thickness in the range 150 to 2000 Å (i.e. for all wall structures).

The surface roughness and inclusion theories of coercive force outlined in this paper have ignored the magnetocrystalline anisotropy and have assumed that the films are unstressed. Introduction of these factors would be expected to cause an increase of the domain wall energy and hence of the domain coercive force. These effects would be expected to be greatest at the extremes of the composition range, and their inclusion in the theoretical treatment would probably lead to improved agreement with the observed compositional dependence.

The confusion existing in some of the observed experimental results is undoubtedly due to the different conditions under which different experimenters worked, with the result that different mechanisms were important to differing extents. It is also not clear how the combination of the various contributions to the coercive force is to be made theoretically if the contributions are correlated. However, if the mechanisms are independent, the resultant coercive force should be the square root of the sum of the squares of the various components.

5. Conclusion

From the work described, it can be seen that there are many aspects of domain coercive force in thin magnetic films which have not yet been adequately investigated either experimentally or theoretically. The most obvious of these is the variation of coercive force with measurement temperature. It is however clear – although perhaps the final relations have still to be established – that the domain coercive force can arise from at least three possible causes depending on the preparation conditions. These are the surface roughness of the film, inclusions and other inhomogeneities in the film, and, in polycrystalline films, the magnetisation ripple. It is however uncertain as to how the components due to the various contributions should be combined.

Acknowledgements

The authors are grateful to Mr C. E. Fuller for his interest and constructive criticism and to Mr A. B. Elkins for assistance with the preparation of figures.

References

1. H. W. FULLER and M. E. HALE, *J. Appl. Phys.* **31** (1960) 238.
2. E. FUCHS, *Z. Angew. Phys.* **14** (1962) 203.
3. M. S. BLOIS, *J. Appl. Phys.* **26** (1955) 975.
4. D. O. SMITH, Conf. Magnetism and Magnetic Materials (Boston, October 1956), p. 625.
5. J. I. RAFFEL, *J. Appl. Phys.* **30** (1959) 605.
6. A. V. POHM and E. A. MITCHELL, *Trans. IRE* **9** (1960) 308.
7. E. M. BRADLEY, *J. Brit. IRE* **20** (1960) 765.
8. R. V. PEACOCK, *Brit Comm. and Electron.* **8** (1961) 436.
9. M. PRUTTON, "Thin Ferromagnetic Films" (Butterworth, 1964).
10. L. NÉEL, *Compt. Rend.* **241** (1955) 533.
11. E. E. HUBER, D. O. SMITH and J. B. GOODENOUGH, *J. Appl. Phys.* **29** (1958) 294.
12. S. MIDDELHOEK, *J. Appl. Phys.* **34** (1963) 1054.
13. M. PRUTTON, *Phil. Mag.* **5** (1960) 625.
14. E. FELDTKELLER, *Z. Angew. Phys.* **15** (1963) 206.
15. J. C. BRICE, *Brit. J. Appl. Phys.* **16** (1965) 1523.
16. L. NÉEL, *J. Phys. Rad.* **17** (1956) 250.
17. R. E. BEHRINGER and R. S. SMITH, *J. Franklin. Inst.* **272** (1961) 14.
18. H. ROTHER, *Z. Physik* **168** (1963) 283.
19. R. J. JOENK, IBM Research Report RC-1281 (1964).
20. H. HOFFMANN, *J. Appl. Phys.* **35** (1964) 1790.
21. L. NÉEL, *Annales de L'Universite de Grenoble* (1945-46) 299.
22. L. NÉEL, *Cahiers de Physique* **25** (1944) 1.
23. L. J. DIJKSTRA and C. WERT, *Phys. Rev.* **79** (1950) 979.
24. H. D. DIETZE, *J. Phys. Soc. Japan* **17** (1962) Suppl. B-1, 633.
25. H. D. DIETZE, *Phys. Kondens. Materie* **2** (1964) 117.

26. W. D. NIX and R. A. HUGGINS, *Phys. Rev.* **135** (1964) A406.
27. R. H. WADE, *Phil. Mag.* **10** (1964) 49.
28. R. COLLETTE, *J. Appl. Phys.* **35** (1964) 3294.
29. W. F. BROWN and A. E. La BONTE, *J. Appl. Phys.* **36** (1965) 1380.
30. M. ONDRIS and Z. FRAIT, *Czech. J. Phys.* **B11** (1961) 883.
31. C. KITTEL, *Phys. Rev.* **70** (1946) 965.
32. J. A. CUNDALL and A. P. KING, Proc. Int. Conf. Magnetism (Nottingham, 1964) p. 847.
33. W. T. SIEGLE and W. R. BEAM, *J. Appl. Phys.* **36** (1965) 1721.
34. H. L. PINCH and A. A. PINTO, *J. Appl. Phys.* **35** (1964) Part II, 828.
35. B. LEWIS, *Brit. J. Appl. Phys.* **15** (1964) 531.
36. H. HOFFMANN, *Z. Angew. Phys.* **18** (1965) 499.
37. A. BALTZ, Proc. Int. Conf. Magnetism (Nottingham, 1964) p. 845.
38. C. H. TOLMAN and P. E. OBERG, Proc. Intermag. Conf. (New York, American Inst. of Elec. Engineers, 1963) Paper 12.3.
39. J. C. BRICE, *Brit. J. Appl. Phys.* **16** (1965) 965.
40. J. A. CUNDALL and A. P. KING, to be published.
41. H. ROTHER, *Z. Physik.* **179** (1964) 229.
42. M. TAKAHASHI, D. WATANABE, T. KONO and S. OGAWA, *J. Phys. Soc. Japan* **15** (1960) 1351.
43. H. WIEDENMANN and H. HOFFMANN, *Z. Angew. Phys.* **18** (1965) 502.
44. S. G. FLEET, Mullard Res. Lab. Report No. 466 (March, 1963).
45. J. H. ENGELMAN and A. J. HARDWICK, *Proc. 9th Nat. Vac. Symp.* (1962) 100.
46. J. C. BRICE and U. PICK, *Vacuum* **14** (1964) 395.
47. J. C. LLOYD and R. S. SMITH, *J. Appl. Phys.* **30** (1959) 274S.
48. I. W. WOLF, *J. Appl. Phys.* **33** (1962) 1152S.
49. J. C. LLOYD and R. S. SMITH, *Canad. J. Phys.* **40** (1962) 454.
50. Y. UEHARA, *Jap. J. Appl. Phys.* **2** (1963) 451.
51. L. REIMER, *Z. Naturforschg.* **11a** (1956) 649.
52. W. RUSKE, *Ann. Physik.* **2** (1958) 274.
53. E. M. BRADLEY and M. PRUTTON, *J. Electronics and Control* **6** (1959) 81.
54. C. O. TILLER and G. W. CLARK, *Phys. Rev.* **110** (1958) 583.
55. K. H. BEHRNDT and F. S. MADDOCKS, *J. Appl. Phys.* **30** (1959) 276S.
56. K. H. BEHRNDT, *J. Appl. Phys.* **33** (1962) 193.
57. F. B. HUMPHREY, *J. Appl. Phys.* **34** (1963) 1067.
58. K. ZAVETA, *Czech. J. Phys.* **5** (1956) 473.
59. S. METHFESSEL, S. MIDDELHOEK and H. THOMAS, *IBM J. Research Devel.* **4** (1960) 96.
60. J. C. BRICE and U. PICK, *Brit. J. Appl. Phys.* **16** (1965) 565.
61. J. F. FREEDMAN, *J. Appl. Phys.* **36** (1965) 964.
62. J. D. BLADES, *J. Appl. Phys.* **30** (1959) 260S.
63. W. HELLENTHAL, *Z. Naturforschg.* **14a** (1959) 722.
64. H. WIEHL, *Z. Angew. Phys.* **18** (1965) 541.
65. LFE Electronics Research in Ferromagnetics Report No. 979-A2 (1961-62).
66. J. C. BRICE and U. PICK, unpublished.
67. W. J. SCHEULE, *J. Appl. Phys.* **35** (1964) 2558.
68. G. BATE, D. E. SPELIOTIS, J. K. ALSTAD and J. R. MORRISON, Proc. Int. Conf. Magnetism (Nottingham, 1964) p. 816.
69. J. RAFFEL and D. O. SMITH, Proc. Int. Conf. Information Processing (UNESCO Paris, 1959) p. 447.
70. G. R. ZELLARS, S. L. PAYNE, J. D. MORRIS and R. L. KIPP, *Trans. AIME* **215** (1959) 181.
71. R. J. HERITAGE, A. S. YOUNG and I. B. BOTT, *Brit. J. Appl. Phys.* **14** (1963) 439.
72. J. C. BRICE and U. PICK, *J. Sci. Instrum.* **41** (1964) 633.
73. M. PRUTTON, *Brit. J. Appl. Phys.* **15** (1964) 815.
74. T. S. CROWTHER, *J. Appl. Phys.* **34** (1963) 580.
75. R. W. OLMEN and S. M. RUBENS, *J. Appl. Phys.* **33** (1962) 1107S.
76. A. VAN ITTERBEEK and A. DUPRÉ, *J. Phys. Rad.* **19** (1958) 113.
77. A. A. HIRSCH, "Electric and Magnetic Properties of Thin Metallic Layers" (Leuven, 1961) p. 128.
78. P. HULYER, Mullard Res. Lab. Report No. 505 (April, 1964).
79. E. W. LEE, *Rep. Prog. Physics* **18** (1955) 184.